Interaction of Hydrophobically Modified Polymers and Surfactant Lamellar Phase

Bing-Shiou Yang,† Jyotsana Lal,‡ Philippe Richetti,§ Carlos M. Marques,§ William B. Russel,† and Robert K. Prud'homme*,†

Department of Chemical Engineering, Princeton University, Princeton, New Jersey 08544-5263, Intense Pulsed Neutron Source, Argonne National Laboratory, Argonne, Illinois 60439, and CNRS/Rhodia, Complex Fluids Laboratory UMR166, Cranbury, New Jersey 08512-7500

Received October 2, 2000. In Final Form: February 13, 2001

We investigate the effect of polysoaps on the phase behavior and membrane elastic properties of the lyotropic lamellar (L_α) phase of the nonionic surfactant penta(ethylene glycol) dodecyl ether ($C_{12}E_5$). The polysoap is a hydrophobically modified polymer (hm-polymer) with *n*-alkyl side groups randomly grafted to a polyacrylate (PAA) backbone. The membrane properties are extracted from small-angle neutron scattering data based on a model developed by Nallet et al. and the excess area method developed by Roux et al. The phase behavior, membrane rigidity, compression modulus, and bilayer mean bending modulus are found to be independent of molecular weight, polydispersity, and hydrophobe length of hm-polymers. The rigidity and compression moduli of membranes increase with increasing polymer concentration and hydrophobe substitution level. A minimum hydrophobic interaction strength (combination of hydrophobe length and hydrophobe substitution level) is required to produce single phase polysoap/lamellar surfactant systems. A scaling model is proposed that defines the boundaries between homogeneous and biphasic solutions based on two criteria: (1) the surface coverage of chain segments between hydrophobes (i.e. blobs) must be less than the available membrane area and (2) the interlamellar spacing must be larger than the blob size. This simple model captures the essential features of the phase diagrams.

I. Introduction

Surfactants can self-assemble into a host of different mesophase structures: vesicles, rods, lamellar sheets, and bicontinuous cubic arrays. The length scales of these structures are comparable to the sizes of many water-soluble polymers. Mixtures of these surfactants and polymers, therefore, display a rich variety of interactions and structural changes. The polymer/surfactant system is of great interest because many industrial products and processes use mixtures of surfactants and polymers. The presence of polymers modifies the properties of the system, e.g., to give a desired rheological response (lubricants) or to stabilize a particular state of surfactant organization (fabric conditioners, etc.). These systems have important applications in material science, cosmetics, pharmacology, medicine, and biology. It has been shown both theoretically[1,2] and experimentally[3−6] that the addition of even a relatively small amount of adsorbing polymers markedly affects the microstructure, elastic properties, and stability of the interface via the specific polymer/surfactant interactions. In our previous study, we found the effect of polymer on the bilayer properties to depend on both the molecular structure of the polymer and polymer concentration.[7] Therefore, a desired performance of the bilayer system can be achieved by manipulating the polymer structure and concentration.

An interesting class of adsorbing polymers consists of so-called hydrophobically modified water-soluble polymers (hm-polymers), which have a water-soluble polymer backbone with covalently bound hydrophobic side chains. Typically, the degree of the hydrophobic substitution is low. The effective strength of the hydrophobic binding between the polymer and the surfactant membrane can be varied conveniently by adjusting this level and the hydrophobicity (e.g. the alkyl chain length) of the side chains.[8] A large number of studies have been performed on dilute aqueous mixtures of hm-polymers and surfactants, where an interesting gel formation occurs with micelles[4,9] or vesicles.[10] A hydrophobically modified polyelectrolyte has also been shown to be soluble in a nonionic surfactant lamellar phase, whereas the unmodified polymer of the same molecular weight phase separates from the surfactant phase.[4]

The elastic properties of the lyotropic lamellar phase (L_α) conventionally are characterized by two fundamental smectic elastic constants, bilayer mean bending modulus (κ) and layer compression modulus ($\bar{B}$). Generally the latter is expected to depend on the interaction between bilayers, while the former is not.[11] The variation of these elastic properties upon addition of polymers has been addressed theoretically[12−17] and experimentally.[18,19] However, the

* To whom correspondence should be addressed.
† Princeton University.
‡ Argonne National Laboratory.
§ CNRS/Rhodia.

(1) de Gennes, P. G. *J. Phys. Chem.* **1990**, *94*, 8407.
(2) Brooks, J. T.; Cates, M. E. *J. Chem. Phys.* **1993**, *799* (7), 5467.
(3) Dexter, D. L. *J. Chem. Phys.* **1953**, *21*, 836.
(4) Iliopoulos, I.; Olsson, U. *J. Phys. Chem.* **1994**, *98*, 1500.
(5) Ligoure, C.; Bouglet, G.; Porte, G. *Phys. Rev. Lett.* **1993**, *71* (21), 3600.
(6) Singh, M.; Ober, R.; Kleman, M. *J. Phys. Chem.* **1993**, *97*, 11108.
(7) Yang, Y.; Prud'homme, R. K.; McGrath, K. M.; Richetti, P.; Marques, C. M. *Phys. Rev. Lett.* **1998**, *80* (12), 2729.
(8) Kabalnov, A.; Olsson, U.; Thuresson, K.; Wennerstrom, J. *Langmuir* **1994**, *10*, 4509.
(9) Magny, B.; Lafuma, F.; Iliopoulos, I. *Polymer* **1992**, *33*, 3151.
(10) Sarrazin-Cartalas, A.; Iliopoulos, I.; Audebert, R.; Olsson, U. *Langmuir* **1994**, *10*, 1421.
(11) Roux, D.; Safinya, C. R.; Nallet, F.; *Micelles, Membranes, Microemulsions and Monolayers*; Gelbart, W. M., Ben-Shaul, A., Roux, D., Eds.; Springer-Verlag: New York, 1994.
(12) Lipowsky, R. *Europhys. Lett.* **1995**, *30*, 197.
(13) Radlinska, E. Z.; Gulik-Krzywicki, T.; Lafuma, F.; Langevin, D.; Urbach, W.; Williams, C. E.; Ober, R. *Phys. Rev. Lett.* **1995**, *74*, 4237.

10.1021/la001391y CCC: $20.00
Published on Web 08/24/2001

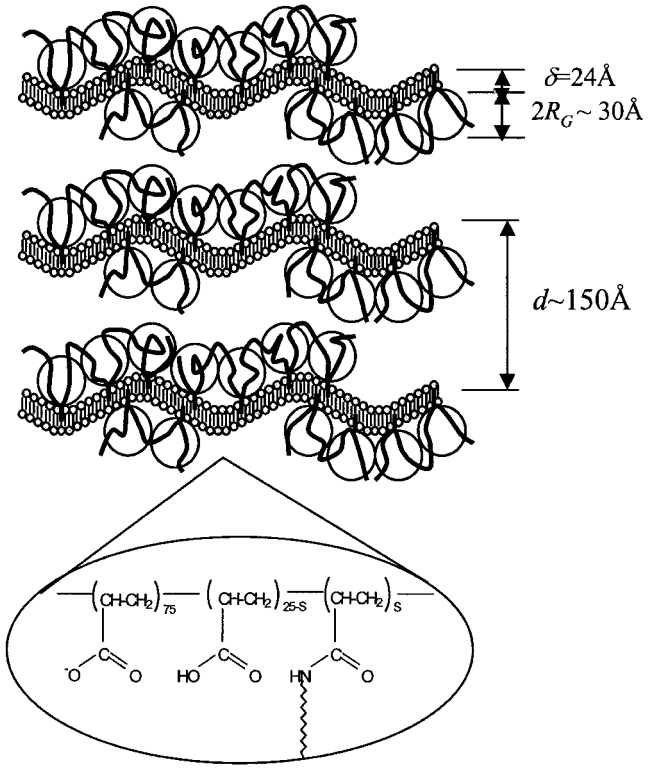

Figure 1. Sketch of the anticipated structure of the mixture of hydrophobically modified polymer and surfactant lamellar phase. The hydrophobic groups along the polymer backbone associate with the membranes forming polymer-doped membranes. The length scales are for $\phi = 0.20$ doped with HMPAA with 3% hydrophobe substitution. The enlarged picture is the chemical composition of hm-polymer with the repeat units distributed randomly. The hydrophobe substitution level *s* and the number outside the repeat units represent molar percentages.

effect of the comblike hydrophobically modified polymers on the membrane properties has not been well characterized.

We have previously characterized the phase behavior of a hydrophobically modified polymer and a nonionic surfactant membrane system.[7] If the radius of gyration of the polymer is comparable to or greater than one-half the interlamellar distance, phase separation generally occurs. Thus, hm-polymers with too few hydrophobic groups along the water-soluble backbone insert themselves into the bilayer stack and reduce the monophasic lamellar domain and induce two coexisting lamellar phases $L_{\alpha 1}$/$L_{\alpha 2}$. Figure 1 sketches the anticipated structure of the hydrophobically modified polymer within the surfactant lamellar phase. The aim of this paper is to study systematically the effect of surface coverage, molecular weight, polydispersity, hydrophobe length, and hydrophobe substitution level on both the phase behavior and the membrane properties of the lamellar phase. The next section describes the materials and the experimental techniques applied in this study. The following section describes the phase behavior for different polymer molecular weights and polydispersities. The neutron scattering results on the effects of surface coverage, molecular weight, polydispersity, hydrophobe length, and hydrophobe substitution level on the surfactant membrane properties are addressed in section IV. The final section highlights the main conclusions.

II. Experimental Section

Systems and Materials. The surfactant lamellar phase consists of the nonionic surfactant penta(ethylene glycol) dodecyl ether ($C_{12}E_5$; >99%, Nikko Chemical Co. Ltd.) and 1-hexanol (>99%, Fluka), used as received. Pure $C_{12}E_5$/water mixtures have a wide L_α phase region at 60 °C, spanning membrane volume fractions ϕ from as low as 0.005 to on the order of unity.[20] Adding hexanol to the membrane reduces the rigidity[21] and extends the wide lamellar range of the phase diagram to room temperature. The $C_{12}E_5$/hexanol molar ratio in all of our samples is fixed at 1:1.43, which reduces the membrane rigidity to $O(k_BT)$.[21] The solvent phase is 0.1 M $NaCl_{(aq)}$. For neutron scattering experiments, the H_2O is replaced by D_2O (Cambridge Isotope Laboratories, Inc.) at the same volume fraction. The phase boundaries are known to shift on the order of 1−3 °C for the substitution of D_2O for H_2O.[22] The neutron scattering experiments on the D_2O samples are conducted in compositions that are 5−7 °C from the phase boundary for the H_2O samples; in addition, the D_2O samples for neutron scattering were confirmed to be in the lamellar phase regime by birefringence. The presence of salt in the solution effectively screens the electrostatic interactions of the added anionic polymers, reducing the Debye length l_D to 10 Å. Thus, the hydrophobically modified PAA (HMPAA) can be viewed as an almost neutral chain with an average number of 1900 (for M_w = 140 kg/mol) or 3500 (for M_w = 250 kg/mol) backbone monomers. With the electrostatic repulsion screened, the undulation force is the dominant long-range repulsion.

The hm-polymers were synthesized by grafting onto precursor poly(acrylic acid) alkylamine (*n*-dodecyl (C_{12}), *n*-tetradecyl (C_{14}), or *n*-octadecyl (C_{18})) in the presence of dicyclohexylcarboiimide (DCC), using *n*-methylpyrrolidinone (NMP) as the solvent.[23] This produces a random distribution of the hydrophobic side chains (C_{12}, C_{14}, or C_{18}) along the PAA backbone.[9] Precursor polymers were handled as follows: An aqueous solution of PAA (Aldrich; M_w = 250 kg/mol, $M_w/M_n \sim 2$) was freeze-dried before use. PAA (Polymer Source, Inc; M_n =136 kg/mol; $M_w/M_n = 1.09$) came in powder form and was used without further treatment. Sodium poly(acrylate) polymer was converted to the acid from PAA by diluting the 25 wt % solution NaPAA (Polysciences, Inc.; $M_w \sim$ 140 kg/mol, $M_w/M_n \sim 2$) with distilled water and then passing it through a bed of Amberlite IR-120 Plus acidic cation exchanger (Supelco, Inc.) before freeze-drying. After the grafting reaction, the modified polymers were precipitated from the NMP solvent by adding concentrated NaOH (40 wt % aqueous solution). The degree of polymerization remains the same as for the precursor with the typical structure illustrated in the inset in Figure 1. Sodium acrylate neutralization of 75 ± 1.5 mol % was determined by elemental analysis and hydrophobe substitution levels by ^{1}H NMR. The compositions of the hmPAA samples are listed in Table 1.

Sample Preparation. The samples were prepared by mixing surfactant ($C_{12}E_5$), alcohol (C_6OH), and stock solutions of the hm-polymers by weight in 0.1 M $NaCl_{(H_2O \text{ or } D_2O)}$. In the following, we define the "membrane volume fraction" (ϕ) as the volume of the $C_{12}E_5$ plus C_6OH divided by the total sample volume with the conversion from weight to volume fractions made with the densities (kg/m^3) of 996 ($C_{12}E_5$), 820 (C_6OH), 1105 (D_2O), and 998 (H_2O), neglecting the effect of the added polymers on the solvent density.

Phase Behavior. The phase behavior was studied in a thermal bath (±0.1 °C) with samples contained in sealed vials, by visual

(14) Marques, C.; Fournier, J. *Europhys. Lett.* **1996**, *35*, 361.
(15) Eisenriegler, E.; Hanke, A.; Dietrich, S. *Phys. Rev. E* **1996**, *54*, 1134.
(16) Ficheux, M. F.; Bellocq, A. M.; Nallet, F. *J. Phys. II* **1995**, *5*, 823.
(17) Brooks, J. T.; Marques, C. M.; Cates, M. E. *J. Phys. II* **1991**, *6*, 673.
(18) Bouglet, G.; Ligoure, C.; Bellocq, A. M.; Dufourc, E.; Mosser, G. *Phys. Rev. E* **1998**, *57*, 1.
(19) Joannic, R.; Auvray, L.; Lasic, D. D. *Phys. Rev. Lett.* **1997**, *78*, 3402.
(20) Strey, R.; Schomacker, R.; Roux, D.; Nallet, F.; Olsson, U. *J. Chem. Soc., Faraday Trans.* **1990**, *86* (12), 2253.
(21) Freyssingeas, F.; Nallet, E.; Roux, D. *Langmuir* **1996**, *12*, 6028.
(22) Hayter, J. B.; Zalauf, M. *Colloid Polym. Sci.* **1982**, *260*, 1023−1028.
(23) Wang, T. K.; Iliopoulos, I.; Audebert, R. *Polym. Bull.* **1988**, *20*, 577.

Table 1. Details of Hydrophobically Modified Polymers

name (abbreviation)	M_w (kg/mol)	M_w/M_n	hydrophobe substitution level (mol %)	hydrophobe length
HMPAA3%250kpoC$_{14}$	250	2	3	C$_{14}$
HMPAA3%140kpoC$_{14}$	140	2	3	C$_{14}$
HMPAA3%140kmoC$_{14}$	140	1.13	3	C$_{14}$
HMPAA3%250kpoC$_{12}$	250	2	3	C$_{12}$
HMPAA3%250kpoC$_{18}$	250	2	3	C$_{18}$
HMPAA1.5%250kpoC$_{14}$	250	2	1.5	C$_{14}$
HMPAA1%250kpoC$_{14}$	250	2	1	C$_{14}$
HMPAA0.8%250kpoC$_{14}$	250	2	0.8	C$_{14}$

inspection in transmitted light, in scattered light, and by observation between crossed polarizers. The lamellar phase (L_α) is optically anisotropic (i.e. birefringence). The sponge phase (L_3) is optically clear and isotropic. The coexisting lamellar phases, $L_{\alpha1}/L_{\alpha2}$, appear turbid under natural light and show an interface between two birefringent phases after centrifugation.

Small-Angle Neutron Scattering (SANS). The small-angle neutron scattering experiments were performed at Argonne National Laboratory at Argonne, IL, with the time-of-flight small-angle diffractometer (SAD). The wave vector (q) varied from 0.005 to 0.35 Å^{-1}. Samples were held in 1 mm path length quartz cells. The data are processed according to the standard procedures, including the subtraction of scattering from the solvent as background and the empty cell contributions. The incoherent scattering of the sample is removed by subtracting the constant background signal at $q \geq 0.3$ Å^{-1} from the data. We have performed SANS experiments on solutions of the hm-polymers without surfactant in 0.1 M $NaCl_{(D_2O)}$ at polymer concentrations corresponding to those used in this study. The scattering intensity from the hm-polymers was 1000 times less than that from the surfactant membrane in the q range of the diffraction peak. Particular attention has been paid to maintaining the lamellar samples in a polycrystalline state to obtain a powder-average scattering intensity. Prior to every neutron scattering run, samples were quenched to preserve a small domain size by first raising the temperature into the isotropic sponge phase range and then quickly immersing in a water bath at $T = 25$ °C. Isotropic 2D spectra obtained in duplicate runs indicated no sensitivity of the d-spacing to details of quenching.

III. Effect of hm-Polymer on Phase Behavior

The phase diagram of the pure surfactant/hexanol reference solution, $C_{12}E_5/C_6OH$/0.1 M $NaCl_{(aq)}$, over the temperature range of 1−50 °C was characterized in our previous study.[24] A wide monophasic L_α domain exists at room temperature for $\phi > 0.062$, indicating a maximum interlamellar distance of about 400 Å. At higher temperature the L_3 phase starts at $\phi \approx 0.059$. At lower volume fraction, the system separates into lamellar and isotropic phases. With increasing temperature the reference solution exhibits a similar sequence of phase transitions as the binary $C_{12}E_5$/water solution,[20] between micellar (L_1), lamellar (L_α), and sponge (L_3) phases. However, all transition temperatures occur about 50 °C lower than for the binary mixture, providing a more convenient system for this study.

Sufficiently strong hydrophobic interactions between the polymer and membrane are required to incorporate poly(sodium acrylate) into the membrane interlamellar spaces. Figure 2 shows the effect of hydrophobe substitution level on the monophasic L_α solution at fixed polymer concentration $C_p = 0.2$ wt % and 25 °C. At a specific hydrophobe substitution level, e.g. 0.8 mol % or higher in Figure 2, polymers of high molecular weight can be solubilized in the surfactant mesophase, forming homogeneous, stable L_α phases over a range of membrane volume fractions. At sufficiently high membrane volume fraction, the doped lamellar phase always phase-separates into two coexisting lamellar phases, $L_{\alpha1}/L_{\alpha2}$, whereas at low membrane volume fractions an isotropic solution coexists with the lamellar phase, which we note as L_α/L_p. This limited miscibility of hm-polymers into the lamellar phase can be explained by the following two criteria: (1) surface coverage of blobs < membrane area available and (2) interlamellar spacing (d) > blob size (ξ). As the membrane volume fraction is decreased at a certain hydrophobe substitution level and polymer concentration, the maximum surface coverage is eventually reached (criterion 1), causing excess polymer to be rejected into a separate isotropic polymer solution phase (L_p). Alternatively as ϕ increases, the average interlamellar spacing eventually drops below the blob size, forcing the system to phase-separate into two coexisting lamellar phases, $L_{\alpha1}/L_{\alpha2}$ (criterion 2), one of which maintains a separation sufficient to accommodate the polymer, while the other is devoid of polymer.

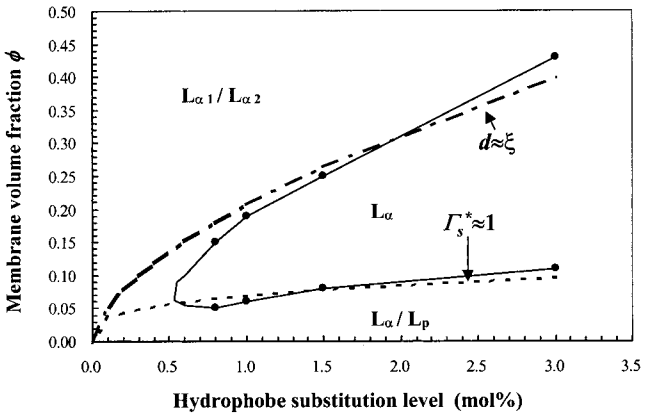

Figure 2. The effect of hydrophobe substitution level on monophasic L_α solution at fixed polymer concentration C_p = 0.2 wt % of HMPAA3%250kpoC$_{14}$ at 25 °C. The miscibility criteria for the two-dimensional overlap concentration (Γ_s^*) for polymer chain of blobs on membrane surface (---), $\phi \sim 0.27s^{3/10}$, and the blob size equaling the spacing between membranes (−-−), $\phi \sim 3.27s^{3/5}$, are best fits of the expected functional forms.

To quantify these criteria we regard anchored hm-polymer as a swollen planar coil of blobs composed of $N_b = M_w s/m_o$ loops with blob size $\xi = l/s^{3/5}$, with m_o (=0.036 kg/mol) being the molecular weight of a statistical segment, m_b being the molecular weight between hydrophobes, s being the hydrophobe substitution level in the mole fraction of backbone monomer units, and l (=5 Å) being the statistical segment length. As we described previously,[7] the anchoring points in the plane of the membrane are not fixed but can relax to their most probable distribution, allowing the characteristic size R of a swollen coil of blobs in two dimensions to assume the equilibrium value of $R = N_b^{3/4}\xi = (M_w/m_b)^{3/4}\xi = (M_w s/m_o)^{3/4}(l/s^{3/5})$. The surface coverage of blobs (per unit volume) is

$$A_{\text{coverage}} \approx \frac{\text{no. of chains}}{\text{volume}} \cdot \frac{\text{area}}{\text{chain}} \approx \left(\frac{C_p N_A}{M_w}\right) R^2 \approx \left(\frac{C_p N_A}{M_w}\right)[(M_w s/m_o)^{3/4}(l/s^{3/5})]^2 \quad (1)$$

where N_A is Avogadro's number. While the total membrane area (per unit volume) is

$$A_{\text{membrane}} \approx \frac{2}{d} \approx \frac{2\phi}{\delta} \quad (2)$$

Therefore, the criterion for full surface coverage is A_{coverage}

(24) Yang, B.-S.; Ph.D. Thesis, Princeton University, Princeton, in preparation.

$\approx A_{\text{membrane}}$, which leads to

$$\phi \approx 1/2(C_p N_A/M_w)\delta l^2 (M_w/m_o)^{3/2} s^{3/10} \quad (3)$$

Criterion 2, the interlamellar spacing is greater than the blob size, $d > \xi$, leads to

$$\phi \approx (\delta/l)s^{3/5} \quad (4)$$

Figure 2 shows that these two scaling relations conform well with the experimental data with values for the prefactors given in the caption, which differ only modestly from the expected values of $\delta/l = 4.7$ and $1/2(C_p N_A/M_w)\delta l^2 (M_w/m_o)^{3/2} = 0.84$. Since surfactant lamellar phases are not stable below $\phi = 0.05$, the miscible region in the experimental phase diagram closes at the low concentration corner. The scaling relations cross there but are not significant.

Unmodified polymer (PAA) and polymer modified with 0.8 mol % or less of hydrophobes do not produce miscible one-phase systems. The mixture phase separates into a lamellar phase and a polymer-rich isotropic phase, even for very dilute membrane solutions. This phase separation for hydrophobe substitution levels below 0.8 mol % shown in Figure 2 can be explained by criterion (2)—interlamellar spacing is not sufficiently greater than the blob size. The diameter of 340 Å for unmodified PAA with molecular weight of 250 kg/mol[25] is comparable to or larger than the interlamellar spacing (e.g. ≤400 Å for the L_α phase) for $\phi \geq 0.07$ or greater. Therefore, the loss of conformational entropy prevents the polymer confinement in the membrane solution if there is not sufficient hydrophobic interaction between the polymer hydrophobes and the lamellar bilayers. Similar results have been reported for other high molecular weight water-soluble polymers.[26,27]

Figure 3 shows the minimal effect of molecular weight and polydispersity of hydrophobically modified polymers on the phase behavior for $C_{12}E_5/C_6OH$/hm-polymers/0.1 M $NaCl_{(aq)}$ over the temperature range of 1−50 °C. The polymer concentrations are fixed at 0.2 wt % for HMPAA 250 kg/mol (polydisperse) and 140 kg/mol (polydisperse and monodisperse) with 3% substitution of C_{14} hydrophobe. The sequence of phases with increasing temperature follows the trend observed in the pure $C_{12}E_5/H_2O$ system[20] and the reference system,[24] corresponding to microstructures in which the mean curvature of the surfactant bilayer decreases monotonically.[28,29] All samples exhibit a similar sequence of phase transitions between micellar solution (L_1), L_α, and L_3, from low to high temperatures. Their roughly horizontal phase boundaries in a moderate concentration range ($0.10 < \phi < 0.50$) mean that the stability is insensitive to the membrane volume fraction.

For these three systems doped with HMPAAs with different molecular weight and polydispersity at equal polymer concentrations ($C_p = 0.2$ wt %), hydrophobe length (C_{14}), and hydrophobe substitution level (3 mol %), the transition between L_α and L_3 occurs in a very similar temperature range (within the range of 30−36 °C). Thus, the molecular weight and polydispersity of the HMPAAs do not affect the spontaneous curvature of the bilayer film significantly. We interpret this to mean that *the phase behavior is determined by the average molecular weight*

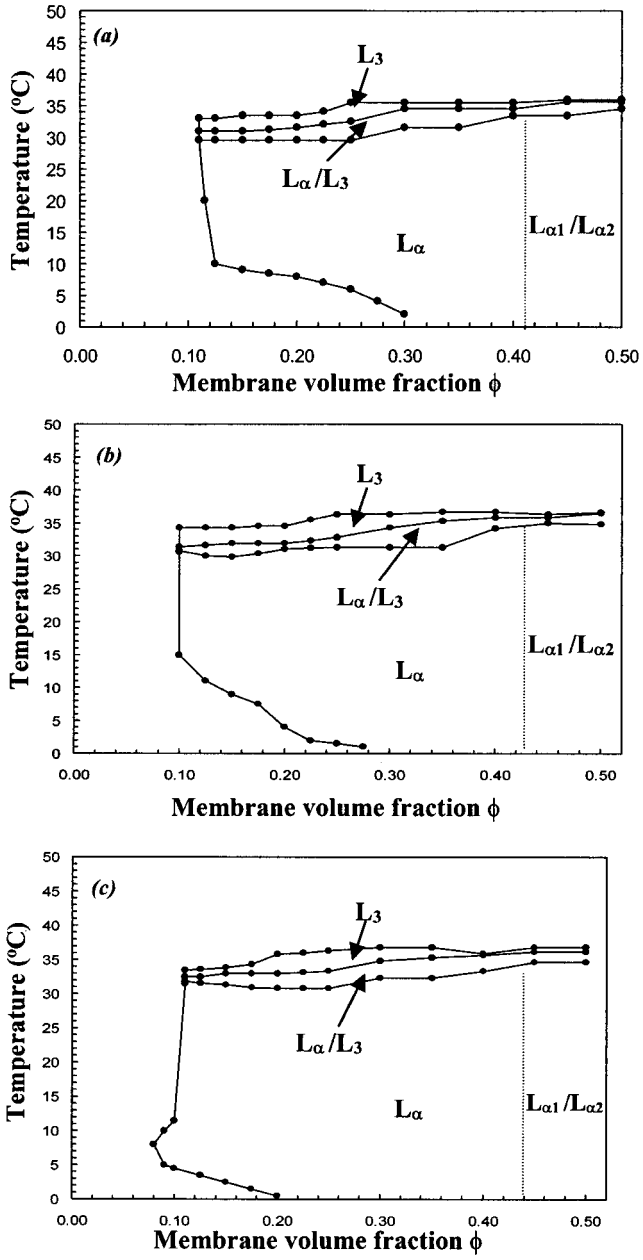

Figure 3. Phase diagram of HMPAA-doped membrane systems: (a) with HMPAA3%250kpoC_{14}, (b) with HMPAA3%140kpoC_{14}, and (c) with HMPAA3%140kmoC_{14}.

(i.e. "loop size") between hydrophobic anchoring sites. The connectivity of the long polymer backbone has only a weak effect, since chains having 57−105 loops display similar phase behavior. However, a forthcoming study of hm-polymers with only 3−13 loops per chain does show a dependence on the number of loops,[30] which appears to indicate an effect of finite chain length seen in many polymer properties.

IV. Neutron Scattering Studies of Membrane Properties

Small-angle neutron scattering allows us to measure the elastic properties of the membranes in the lamellar phase and the effect of hm-polymers on membrane elastic constants. Two primary features of intensity *I(q)*, of a

(25) Brandrup, J.; Immergut, E. H.; *Polymer Handbook*, 3rd ed.; John Wiley and Sons: New York, 1989.
(26) Bagger-Jorgensen, H.; Olsson, U. *Langmuir* **1995**, *11*, 1934.
(27) Déme, B.; Dubois, M.; Zemb, T.; Cabane, B. *J. Phys. Chem.* **1996**, *100*, 3828−3838.
(28) Strey, R. *Colloid Polym. Sci.* **1994**, *272*, 1005.
(29) Olsson, U.; Wennerstrom, H. *Adv. Colloid Interface Sci.* **1994**, *49*, 113.

(30) Yang, B.-S.; Lal, J.; Kohn, J.; Huang, J. S.; Russel, W. B.; Prud'homme, R. K., to be submitted to *Langmuir*.

lamellar phase depend on interlamellar interactions.[31,32] With strong electrostatic repulsions $I(q\rightarrow 0)$ is low, the correlation peaks are sharp, and several orders of diffraction can be observed. With weak repulsive interactions such as the undulation force, $I(q\rightarrow 0)$ is relatively high and usually only a broad first-order peak remains and becomes broader with decreasing membrane volume fraction.[33] The correlations between the lamellae are known to produce a Bragg peak at $q_o = 2\pi/d$ with a power law singularity, $I(q) \propto |q - q_o|^{-1+\eta}$, with the Caillé constant η defined as[34]

$$\eta = \frac{q_o^2 k_B T}{8\pi\sqrt{\kappa \bar{B}/d}} \tag{5}$$

where d is the interlamellar spacing, κ is in units of k_BT, and $\bar{B}$ is in units of k_BT per volume. Thus structural and thermodynamic properties can be obtained from the positions and shapes of the Bragg peaks, respectively.[11] Therefore, the spectra will be normalized on the peak values $I(q_o)$ and q_o and attention will be focused on the shape of the peak characterized by η.

In this paper, the full SANS spectra are fitted according to a model developed by Nallet et al.,[35] which results from the convolution of the thermally broadened shape for a finite-size lamellar domain with an instrumental resolution function with a Gaussian component (of width Δq). This model expresses the scattering intensity of the lamellar phase as

$$I(q) \approx q^{-2} P(q) S(q) \tag{6}$$

where $P(q)$ and $S(q)$ are the form factor and the structure factor, respectively. The q^{-2} dependence arises from the powder average for randomly oriented lamellar domains. The form factor is given by (ref 34, eq 19)

$$P(q) = \frac{2\Delta\rho^2}{q^2}[1 - \cos(q\delta)e^{-q^2\sigma^2/2}] \tag{7}$$

with $\Delta\rho$ being the contrast between the hydrophobic part of the bilayer and the solvent (including the hydrated part of the bilayer and the polymer) and σ being the width of the Gaussian distribution of the neutron scattering length density. Parameters used in the fitting of the data were $\sigma = 4.5$ Å, $\Delta\rho = 0.0035-0.0038$ cm^{-2}, and $\delta = 24$ Å. The structure factor $S(q)$ given by Nallet et al. (ref 34, eq 14) was used where the instrumental resolution effect is included by convolution with a Gaussian distribution with width Δq

$$\Delta q = 0.0010968 + 0.012786q + 0.41845q^2 - 2.651q^3 + 7.0433q^4 - 6.947q^5 \tag{8}$$

which includes the effects of collimation and detector size.[36−38] The parameters in eq 8 have been reported in Bhatia's work performed on the same beam line.[38] Figure 4 exemplifies the fitting on the system of $C_{12}E_5/C_6OH$/0.1 M $NaCl_{(D_2O)}$ with $\phi = 0.20$. The model fits the experimental data except at very low q. The increased scattering intensity observed at low q arises from scattering by finite-sized lamellar domains. The Nallet model considers scattering from randomly oriented domains that are assumed to be infinite in extent and, therefore, the low q behavior includes only contributions from the osmotic compressibility ($\bar{B}$). The best fit of the data was determined using the value for the membrane thickness of $\delta = 24$ Å. This is confirmed from the analysis of the high-q region of the neutron scattering spectra. Plotting $q^4I(q)$ highlights the maximum in form factor (once the incoherent background scattering has been subtracted), from which we estimate a bilayer thickness $\delta = 24 \pm 2$ Å that is independent of polymer molecular weight, polydispersity, and polymer concentration.[39]

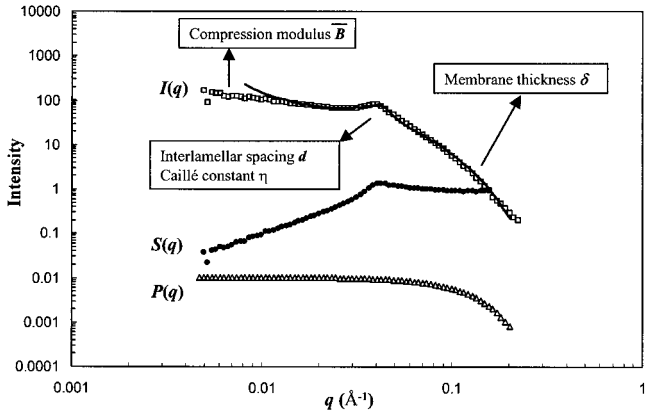

Figure 4. Scattering intensity $I(q)$ (□), structure factor $S(q) = q^2I(q)/P(q)$ (●), and form factor $P(q)$ from eq 7 (△) of $C_{12}E_5/C_6OH$/0.1 M $NaCl_{(aq)}$ at $\phi = 0.20$ and $I(q)$ from the model of Nallet et al.[35] (—) with the fitting parameters shown in Table 2.

The compressibility of the membrane stack is reflected in the low q behavior of the structure factor $S(q)$ obtained from the experimental scattering intensity $I(q)$ from eq 6. The structure factor $S(q)$, form factor $P(q)$, and scattering intensity $I(q)$ are shown in Figure 4. In the presence of thermal fluctuations, higher order Bragg peaks are smoothed out[35] and $S(q)$ reaches its asymptotic value of unity at high q. Such a behavior is common for disordered systems or liquids. The low q limit of $S(q)$ indicates the compressibility of the system but cannot be determined quantitatively due to the limited range of q accessible.

Effect of Polymer Concentration. The normalized SANS spectra of the lamellar phase doped with HMPAA3%140kpoC_{14} at $\phi = 0.20$ for different polymer concentrations in Figure 5 have two important features. The first is the reduction in the width of the Bragg peak with hm-polymer addition. This indicates a decrease in the Caillé constant η (eq 5) and, therefore, an increase in rigidity (i.e. the product $\kappa\bar{B}$)[7] and, second, changes in the diffuse scattering at small q, which is particularly pronounced with little or no HMPAA. The small q limit, $I(q\rightarrow 0)$, reflects the layer compression modulus $\bar{B}$, which depends on the bilayer/bilayer interaction as mentioned above. The stronger the repulsion between bilayers, the more the positional fluctuations are suppressed. Since $I(q\rightarrow 0) \propto 1/\bar{B}$, reduced scattering at low angles corresponds

(31) Roux, D.; Safinya, C. R. *J. Phys. Fr.* **1988**, *49*, 307.
(32) Morris, C. *J. Membr. Biol.* **1990**, *113*, 93−107.
(33) Bagger-Jorgensen, H.; Coppola, L.; Thuresson, K.; Olsson, U.; Mortensen, K. *Langmuir* **1997**, *13*, 4204.
(34) Caillé, A.; Heb, C. R. *C. R. Acad. Sci. B* **1972**, *274*, 1733.
(35) Nallet, F.; Laversanne, R.; Roux, D. *J. Phys. II Fr.* **1993**, *3*, 487.
(36) Thiyagarajan, P.; Epperson, J. E.; Crawford, R. K.; Carpenter, J. M.; Klipper, T. E.; Wozniak, D. G. *J. Appl. Crystallogr.* **1997**, *30*, 280−293.
(37) Pedersen, J. S.; Posselt, D.; Mortensen, K. *J. Appl. Crystallogr.* **1990**, *23*, 321−333.
(38) Bhatia, S. R.; Ph.D. Thesis, Princeton University, Princeton, **2000**.
(39) Yang, B.-S.; Lal, J.; Mihailescu, M.; Monkenbusch, M.; Richter, D.; Huang, J. S.; Russel, W. B.; Prud'homme, R. K. In *Lecture Notes in Physics: Neutron Spin−Echo Spectroscopy−future aspects and applications*; Springer: New York, **2000**.

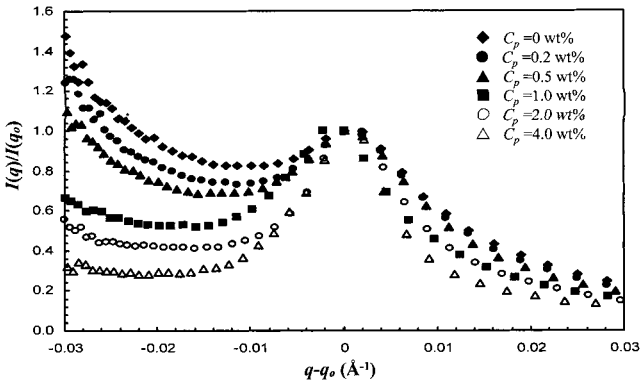

Figure 5. Scattering data normalized with respect to the positions and intensities at the peak for the lamellar phase at $\phi = 0.20$ and different concentrations of HMPAA3%140kpoC$_{14}$.

to an increase of $\bar{B}$ with increasing polymer concentration, though a quantitative characterization is not possible.

Effect of Surface Coverage. Increasing the polymer concentration at constant membrane volume fraction increases the polymer surface coverage. We explored changing membrane concentration at constant coverage (i.e., constant C_p/ϕ) for the polymer HMPAA3%250kpoC$_{14}$ at $\phi = 0.15-0.30$.[24] Both the Bragg peak width and the small q behavior for the four samples differ even with the same surface coverage. Samples with three other surface coverages ($C_p/\phi = 0$, 0.1, 0.125) within the homogeneous lamellar phase region exhibit similar behavior. The fitted values of the Callié constant η at specific C_p/ϕ decrease with increasing membrane volume fraction and increasing coverage. Thus, at least the compressibility $\bar{B}$ depends on volume fraction as well as coverage and the bending modulus κ may also.

Effect of Molecular Weight and Polydispersity. In this part, we employed HMPAA3%250kpoC$_{14}$, HMPAA3%140kpoC$_{14}$, and HMPAA3%140kmoC$_{14}$. The dependence of η on polymer concentration for these three polymers in Figure 6 indicates no significant effect of molecular weight or polydispersity. The inserts illustrate more clearly the minimal effect of hm-PAA molecular weight and polydispersity for $\phi = 0.20$. For $C_p = 0.2$ wt % (Figure 6a) or 2 wt % (Figure 6b), the scattering spectrum from these three different hmPAAs are similar, reinforcing the insensitivity to molecular weight and polydispersity.

Since the Caillé constant η contains the product of κ and $\bar{B}$, we turn to the excess area method to separate the membrane stiffness from the interactions that control $\bar{B}$.[40] Upon addition of solvent to the lamellar phase, the periodicity d of the stack of membranes increases. On geometrical grounds (viewing the membranes as rigid objects) a simple law $d \propto 1/\phi$ is expected. However, in the absence of direct, long-range interactions between membranes, a logarithmic correction to this simple dilution law is required, because of the short wavelength fluctuations of the membrane.[41] This correction has been applied to flexible surfactant membranes (i.e., κ on the order of k_BT).[20,21,40,42] According to the theoretical argument and experimental observations, the logarithmic correction is written—for dilute enough lamellar phases—as follows

$$\frac{d\phi}{\delta} = 1 + \frac{1}{4\pi\kappa} \ln\left[\frac{\delta}{\phi b}\sqrt{\frac{32\kappa}{3\pi}}\right] \qquad (9)$$

where b is a microscopic cutoff length that we take as $b = 7$ Å.[7,21] Once κ is obtained from the excess area method then $\bar{B}$ follows from the Caillé constant η.

The evolution of the interlamellar distance d as a function of the membrane volume fraction ϕ was extracted from the position of the first-order Bragg peak position q_o of the small angle neutron scattering spectra as $d = 2\pi/q_o$ at constant hexanol/$C_{12}E_5$ mole ratio (=1.43), temperature (25 °C), and polymer concentration C_p (=0.2 wt %). For these conditions the membrane volume fraction was varied as $0.15 \le \phi \le 0.35$ within the single lamellar phase region (Figure 3c). As the volume fraction increases, the peak

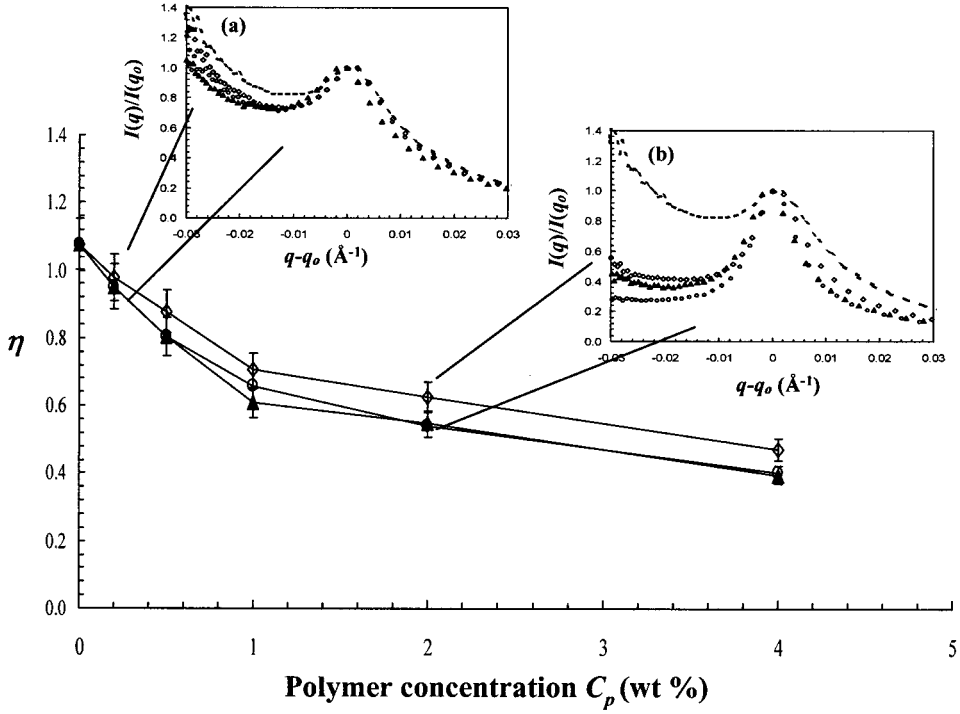

Figure 6. Dependence of Caillé constants η on polymer concentration for HMPAA3%250kpoC$_{14}$ (○), HMPAA3%140kpoC$_{14}$ (▲), and HMPAA3%140kmoC$_{14}$ (◇). The membrane volume fraction ϕ is fixed at 0.20 for all samples. The two enlarged figures are the normalized SANS spectrum for the same systems at (a) $C_p = 0.2$ wt % and (b). $C_p = 2$ wt %.

Table 2. Summary of Fitting Parameters for System $C_{12}E_5/C_6OH$/0.1 M $NaCl_{(D_2O)}$ /hm-polymer; C_p = 0.2 wt%

	no polymer		HMPAA3 %250kpo C14		HMPAA3 %140kpoC 14		HMPAA 3%140k moC14	
ϕ	d (Å)	η	d (Å)	η	d (Å)	η	d (Å)	η
0.15	243.0	1.32	232.0	1.27	220.0	1.15	209.0	1.63
0.20	159.0	1.08	159.4	0.95	155.0	0.95	163.0	0.98
0.25	118.0	0.83	119.0	0.83	121.0	0.81	121.0	0.73
0.30	104.0	0.67	101.6	0.69	99.0	0.67	99.0	0.64
0.35	83.2	0.42	85.3	0.51	85.0	0.55	85.0	0.53
κ (k_BT), eq 9	0.7 ± 0.2		0.9 ± 0.2		0.9 ± 0.2		0.9 ± 0.2	
δ (Å), eq 9	24 ± 2		24 ± 2		24 ± 2		24 ± 2	

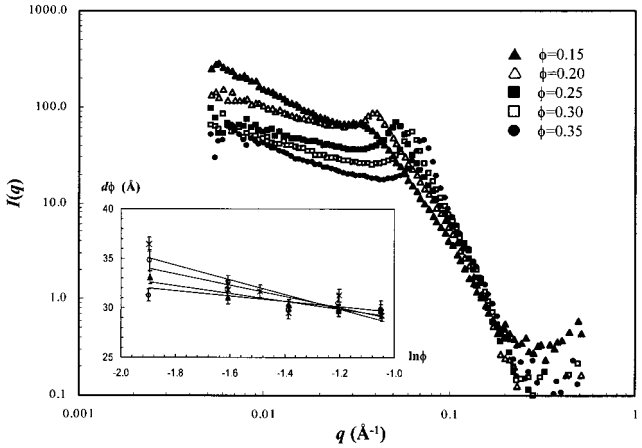

Figure 7. The SANS spectrum for the samples with HMPAA3%140kmoC_{14} (C_p=0.2 wt) at $0.15 \le \phi \le 0.35$. The insert shows the measure values of dϕ vs ln ϕ over the whole dilution range with no polymer (•), HMPAA3%250kpoC_{14} (○), HMPAA3%140kpoC_{14} (▲), and HMPAA3%140kmoC_{14} (◇). The corresponding bending moduli κ and membrane thickness δ are shown in Table 2.

intensity decreases and the position moves to higher q (Figure 7). The insert of Figure 7 displays the measured values of dϕ over the whole dilution range ($0.15 \le \phi \le 0.35$) as a function of ln ϕ. The best fit of the data with eq 9 determines the membrane thickness (δ) and the bending constant (κ) shown in Table 2. The fitted membrane thicknesses (δ) for all systems equal 24 ± 2 Å, which is consistent with the fitted value from Nallet and co-worker's model[35] and indicates that the membrane thickness of the doped lamellar phase does not change with the molecular weight and polydispersity of the hmPAAs. The bending modulus (κ) is about 30% larger with hmPAA than without but within experimental uncertainty is independent of the molecular weight and polydispersity. The dilution at constant polymer concentration results in the polymer surface coverage varying over the dilution series. However, measurements at constant surface coverage (C_p/ϕ) for several values of ϕ produced qualitatively similar results with κ increasing approximately 20% for the series with the same polymer coverage as the sample of C_p = 0.2 wt % and ϕ = 0.20.

Effect of Hydrophobe Substitution Level and Length. The effect of hydrophobe substitution level in Figure 8 is demonstrated with HMPAA1.5%250kpoC_{14} and HMPAA3%250kpoC_{14} at C_p = 2 wt % and ϕ = 0.20. The breadth of the Bragg peaks and the scattering intensity at low angles decrease as the hydrophobe substitution level increases, indicating that the Caillé constant and the compressibility both decrease (see the inset of Figure 8).

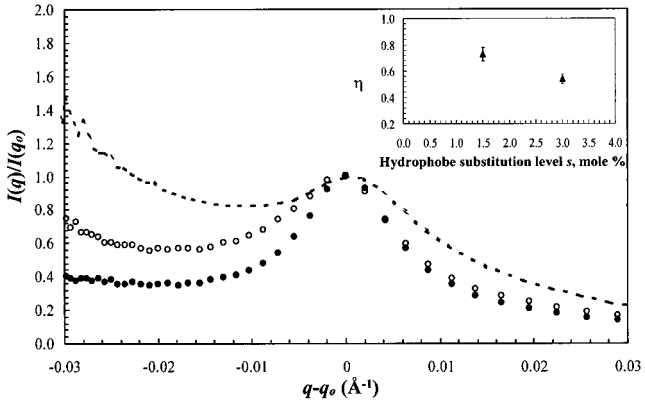

Figure 8. The normalized SANS spectrum with no polymer (---), HMPAA1.5%250kpoC_{14} (○), and HMPAA3%250kpoC_{14} (●) at C_p = 2 wt % and ϕ = 0.20 with the insert showing the corresponding values for η.

In addition to the hmPAA with C_{14} hydrophobe (HMPAA3%250kpoC_{14}), two other hmPAAs with 3% hydrophobe substitution but different hydrophobes (C_{12} and C_{18}), HMPAA3%250kpoC_{12} and HMPAA3%250kpoC_{18}, were also synthesized. Neither the scattering spectra nor the fitted Caillé constants for the three different hydrophobe lengths[24] differ significantly. Though the hydrophobe length does not affect the static membrane properties (rigidity and compressibility) significantly, the effect on the dynamics could be substantial.

V. Conclusion

In this study, we demonstrate systematically the effect of the concentration and structure of hydrophobically modified polymers on the phase behavior and properties of the surfactant lamellar system using direct observation and small angle neutron scattering:

(a) Phase behavior of hm-polymer-doped lamellar systems is essentially independent of polymer molecular weight and polydispersity.

(b) At constant membrane volume fraction with increasing polymer concentration and higher hydrophobe substitution level, membrane rigidity increases and compressibility decreases.

(c) The Caillé constant (η) at constant C_p/ϕ decreases with increasing membrane volume fraction and increasing coverage. Thus, at least the compressibility ($\bar{B}$), and perhaps the bending modulus (κ), depends on volume fraction as well as coverage.

(d) Membrane thickness does not change significantly with polymer concentration, molecular weight, polydispersity, hydrophobe length, and hydrophobe substitution level of hm-polymers with hydrophobe substitution level from 1.5 to 3 mol %.

(e) Molecular weight, polydispersity, and hydrophobe length do not change membrane properties (rigidity and compression modulus) significantly.

(40) Roux, D.; Nallet, F.; Freyssingeas, E.; Porte, G.; Bassereau, P.; Skouri, M.; Marginan, J. *Europhysics Lett.* **1992**, *17* (7), 575.
(41) Helfrich, W.; Servuss, R.-M. *Nuovo Cimento D* **1984**, *3*, 137.
(42) Freyssingeas, E.; Roux, D.; Nallet, F. *J. Phys. Condens. Matter* **1990**, *86* (12), 2253.

(f) Two conditions are needed for the miscibility of strongly anchored hm-polymers and lamellar phase: (1) surface coverage of blobs < membrane area available and (2) interlamellar spacing (d) ≫ blob size (ξ).

These observations are consistent with the concept of each polymer forming a chain of blobs on the surface of the surfactant bilayer. Fluctuations in curvature may require stretching or compression of the chain of blobs anchored on the membrane surface, and fluctuations in interlamellar separation would involve compression of the individual blob from its equilibrium conformation, increasing the free energy and thereby increasing the rigidity and the compression moduli.

LA001391Y